Entanglement and purification transitions in non-Hermitian quantum mechanics

Sarang Gopalakrishnan[1,2] and Michael J. Gullans[3]

[1]*Department of Physics, The Pennsylvania State University, University Park, PA 16802, USA*
[2]*Department of Physics and Astronomy, CUNY College of Staten Island, Staten Island, NY 10314; Physics Program and Initiative for the Theoretical Sciences, The Graduate Center, CUNY, New York, NY 10016, USA*
[3]*Joint Center for Quantum Information and Computer Science, NIST/University of Maryland, College Park, Maryland 20742 USA*

A quantum system subject to continuous measurement and *post-selection* evolves according to a non-Hermitian Hamiltonian. We show that, as one increases the strength of post-selection, this non-Hermitian Hamiltonian can undergo a spectral phase transition. On one side of this phase transition (for weak post-selection) an initially mixed density matrix remains mixed at all times, and an initially unentangled state develops volume-law entanglement; on the other side, an arbitrary initial state approaches a unique pure state with low entanglement. We identify this transition with an exceptional point in the spectrum of the non-Hermitian Hamiltonian, at which PT symmetry is spontaneously broken. We characterize the transition as well as the nontrivial steady state that emerges at late times in the mixed phase using exact diagonalization and an approximate, analytically tractable mean-field theory; these methods yield consistent conclusions.

The dynamics of open quantum systems is a central theme in contemporary many-body physics [1–4]. One can often model open systems as being coupled to Markovian environments, or equivalently as undergoing repeated weak measurements, each involving a new measuring apparatus. The system and the measuring apparatuses are collectively in a pure state. For each specific sequence of measurement outcomes (called a "quantum trajectory" [5]), the system itself is in a pure state, but if one traces over measurement outcomes the system is in a mixed state that evolves according to a Lindblad master equation [6, 7]. Recent work, motivated by quantum circuits, has explored the properties of wavefunctions associated with typical individual trajectories. These single trajectories undergo a phase transition in their entanglement properties as the rate of measurements is increased [8–32]: for weak or sparse measurements, the bipartite entanglement of the system along a typical trajectory grows to a volume law (as it does under purely unitary dynamics); for strong or dense measurements, a typical trajectory has area-law entangled wavefunctions. This "measurement phase transition" has also been interpreted in terms of the ability of the dynamics to hide information in nonlocal correlations that the measurements do not probe [12, 13, 15]. This transition is, however, invisible in the trajectory-averaged evolution of the density matrix under the master equation.

Measurement transitions have been studied, both for *typical* trajectories (where each trajectory is weighted by the Born probability of the measurement outcomes), and for *post-selected* trajectories where one fixes a particular measurement outcome at the outset. The transition that occurs in the latter case is the "forced measurement phase transition" [31] (see also [33–35]), and might belong to a different universality class than that for typical trajectories [31]. Work so far on either transition has assumed some irreducible temporal randomness, in the dynamics or the measurement outcomes. This temporal randomness has been assumed to be central to the physics of the transition [8, 11], but makes it unnatural to address measurement phase transitions from the *spectral* perspective that has proved fruitful for understanding many-body entanglement and chaos [36–38].

In the present work, we show that temporal randomness is not essential to realize measurement-induced entanglement transitions. We study systems in which the time evolution and the measurement outcomes are fixed, so there is a well-defined non-unitary evolution opera-

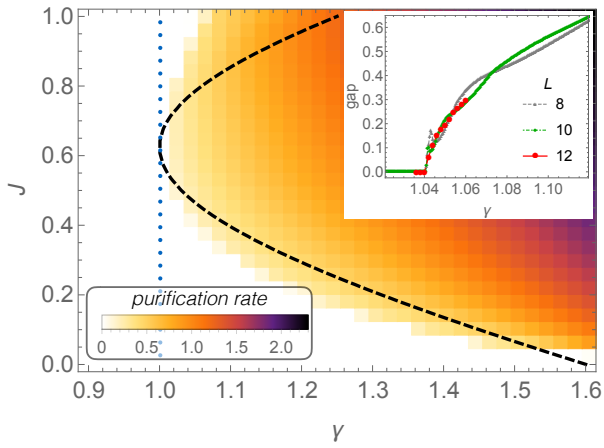

FIG. 1. Phase diagram of purification rate—i.e., the gap between the slowest- and second-slowest decaying eigenvalues of the non-Hermitian Hamiltonian (7)—vs. measurement strength γ and interaction strength J for $h_0 = 1.25$ and $\epsilon = 0$. The dashed line is the mean-field prediction, which is in good agreement with the numerical data (color map) on one-dimensional spin chains. The model is solvable at $\gamma = 1$ (dotted one). Inset: size-dependence of gap for $J = 0.95$.

tor whose spectral properties we can study. We consider a chaotic Ising chain subject to continuous weak measurements of the Pauli operator σ^y on every site. We post-select on the outcome where the weak measurements do not show the spin being in the state $|-y\rangle$. This post-selected dynamics is described by a non-Hermitian Hamiltonian that (apart from a trivial shift on the diagonal) has purely real entries [39]. This non-Hermitian Hamiltonian undergoes a spectral transition: for strong measurements, each eigenvalue of the non-Hermitian Hamiltonian has a distinct imaginary part (decay rate), so any initial state eventually gets projected onto the longest-lived eigenstate, which is area-law entangled; when the measurements are weaker than a certain threshold, all the eigenvalues have the *same* decay rate, so an initially mixed state remains mixed forever. (A related result holds in the volume-law phase of the measurement transitions studied so far: mixed states are exponentially long-lived in system size [12, 30].) Further, an initial product state develops volume-law entanglement. An analogue of this post-selection transition is sharply defined even for few-level systems, and corresponds to an exceptional point [40]. In the many-body case in the thermodynamic limit, the transition is instead due to the coalescence of many exceptional points; surprisingly, the critical measurement strength remains finite and the mixed phase exists as a true phase. We present numerical evidence for this conclusion, prove that it holds along a solvable line of parameters, and develop a mean-field theory of the transition, which works better than one might expect even in one dimension (Fig. 1). We then explore the phenomenology of the mixed phase and transition, and compare them with the random-circuit problem.

Exceptional points have been extensively studied, mostly in the context of few-level systems [40–46]; to our knowledge, it has not previously been observed that exceptional points can occur in the middle of the spectrum for a chaotic strongly interacting system in the thermodynamic limit. We also emphasize that our post-selected "purification transitions" are distinct from phase transitions in the steady-state purity of a density matrix that occurs in some master equation evolutions [47–49]. The master equations associated with the non-Hermitian Hamiltonians we study always have the infinite temperature density matrix as the long-time steady state.

Purification of a two-level system.—We first consider the simplest purification problem, which is that of a two-level system. Consider a master equation with a single jump operator proportional to $(1-\sigma^y)$ [1, 39]. The corresponding non-Hermitian Hamiltonian is $H_{\text{eff}} = H_0 - ib(1-\sigma^y)$. We choose our coordinate system so that $H_0 = \sigma^x$; then $H_{\text{eff}} = M_0 - ib$ where

$$M_0 \equiv \begin{pmatrix} 0 & 1+b \\ 1-b & 0 \end{pmatrix}, \tag{1}$$

and b is real. The characteristic equation of this matrix is $\lambda^2 = 1-b^2$, so when $|b|<1$ the eigenvalues are both real. The eigenvalues collide when $b=1$, leading to an "exceptional point." When $b>1$ both eigenvalues are purely imaginary. M_0 is a classic example of a PT-symmetric non-Hermitian matrix. Such matrices have real spectra, but *nonorthogonal* eigenvectors. In the present example, the (standard) inner product between the two eigenvectors is $|b|$. When $b = 1-\epsilon$, the eigenvectors take the form $|\pm\rangle \approx (1, \pm\sqrt{\epsilon/2})$. At the exceptional point $b=1$ the eigenvectors become parallel, so the matrix ceases to be diagonalizable. For small $\epsilon > 0$, the two eigenvectors are linearly independent and thus span the entire space. However, the expression for a generic vector in this basis [for example $(0,1) = 1/\sqrt{\epsilon}(|+\rangle - |-\rangle)$] involves large coefficients and approximate cancellations.

We consider the dynamics of initially mixed states evolving under this non-Hermitian Hamiltonian, $T = \exp(-iH_{\text{eff}}t)$. For any diagonalizable matrix one can write $T = PDP^{-1}$, where the columns of P are eigenvectors of H_{eff}, and D is a diagonal matrix with entries $e^{-i\lambda_k t}$ where λ_k are the eigenvalues of H_{eff}. We write this expression out in general, using some reference orthonormal basis:

$$\rho \propto [(P^\dagger)^{-1}]_{ij} e^{i\lambda_j^* t} (P^\dagger)_{jk} P_{kl} e^{-i\lambda_l t} (P^{-1})_{lm}. \tag{2}$$

Eq. (2) supports two kinds of behavior. In one regime ($|b|>1$ for the toy model) the λ_k have unequal imaginary parts, and T is (up to normalization) a projector onto the slowest-decaying eigenvector. In the other ($|b|<1$) all the λ_k have the *same* imaginary part, so a mixed state remains mixed. The phase factors in Eq. (2) oscillate, and averaging over oscillations (by going into an appropriate "diagonal ensemble" [37]) yields the time-averaged density matrix

$$\rho_{\text{ss}} \propto [(P^\dagger)^{-1}]_{ij} (P^\dagger)_{jk} P_{kj} (P^{-1})_{jm}. \tag{3}$$

Defining the steady-state purity as $\Pi \equiv \text{Tr}(\rho_{\text{ss}}^2)/(\text{Tr}\rho_{\text{ss}})^2$, one finds that $\Pi = \frac{1}{2}(1+b^2)$. Putting this together with the $|b|>1$ regime, the steady-state purity in this case is a continuous function of b, with a cusp at $b=1$. Precisely at the exceptional point, H_{eff} has only one eigenvector, $(1,0)$. An initial state $|\psi\rangle = (\cos\theta, \sin\theta)$ evolves to the (unnormalized) state $|\psi(t)\rangle = (\cos\theta + it\sin\theta, \sin\theta)$. Thus, any initial state eventually points along the eigenvector, and a mixed state purifies as $1-\Pi(t) \sim 1/t^4$.

Mean-field theory.—The analysis above can be directly extended to a mean-field theory for purification transitions. Consider the non-Hermitian Hamiltonian for N sites i each with a spin-1/2 particle that interacts with external magnetic fields and each other particle:

$$H_{\text{eff}} = \sum_i [h_i \sigma_i^z + g_i \sigma_i^x - i\gamma(1-\sigma_i^y)] + \sum_{ij} J_{ij} \sigma_i^z \sigma_j^z, \tag{4}$$

in which h_i/g_i is a magnetic field in the z/x-direction, J_{ij} is the interaction strength, and γ is the strength of post-

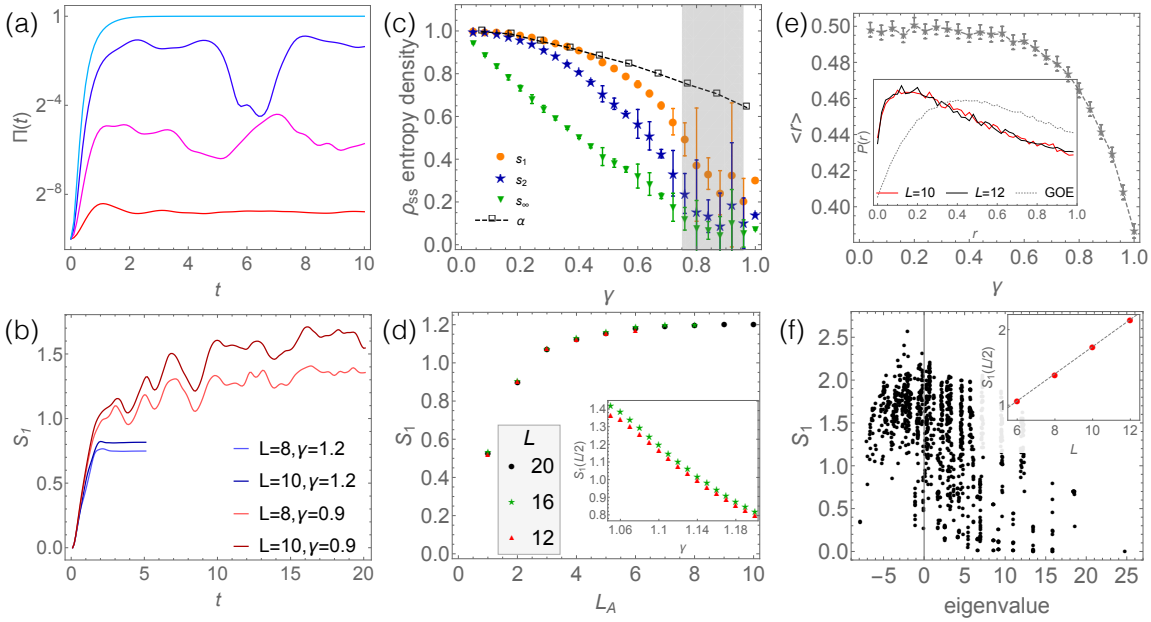

FIG. 2. (a) Dynamics of the purity $\Pi(t)$ of an initially fully mixed state and (b) the bipartite entanglement entropy S_1 of a random initial pure state (averaged over 100 random product states) under the Hamiltonian (4), showing a clear qualitative distinction between the area law/pure and volume law/mixed phases. (c) In the mixed phase, the time-averaged density matrix (see main text) has a finite entropy density that continuously decreases as γ is tuned toward the transition. The quantity α (which is an estimate of the accessible Hilbert space) tracks the Von Neumann entropy density (s_1) for small γ. (d) On the area law side, any initial state converges to the slowest decaying eigenstate, which is area law entangled with (inset) a coefficient that grows as the transition is approached. (e) Eigenvalue statistics in the mixed phase; (inset) the deviation from random-matrix theory seems to persist with system size. (f) Eigenvector entanglement for a single realization at $\gamma = 0.9$. (inset) The mean half-chain eigenvector entanglement grows as a volume law. Panels (a,b,d) are for $\epsilon = 0$; panels (c,e,f) are for $\epsilon = 0.05$, to lift degeneracies in the spectrum and make the problem well-defined. Results are insensitive to the precise choice of ϵ. Error bars in (c,e) denote one standard deviation due to variations over disorder realizations.

selection. Decoupling the interaction yields a Hamiltonian for a single spin subject to a complex field,

$$h_{\text{eff}}(\langle\sigma^z\rangle) = \left(h_i + \sum\nolimits_j J_{ij}\langle\sigma_j^z\rangle\right)\sigma^z + g_i\sigma^x + i\gamma\sigma^y. \quad (5)$$

A self-consistent system can be attained by solving for $\langle\sigma^z\rangle$. For a translation-invariant system, this mean-field theory predicts that the phase transition occurs when

$$g\gamma = g^2 + (h - Jz)^2, \quad (6)$$

where z is the coordination number of each site. This mean-field theory agrees well with numerics even for one-dimensional spin chains, though there are discrepancies at interaction strengths $J \approx 1$ (Fig. 1).

One-dimensional spin chains.—We now turn to numerical results on spin chains evolving under the following non-Hermitian Hamiltonian:

$$H = \sum_i \left[h_i\sigma_i^z + \sigma_i^x - i\gamma(1 - \sigma_i^y) + J\sigma_i^z\sigma_{i+1}^z\right]. \quad (7)$$

We will explore both the translation-invariant model and a model with weak randomness in the longitudinal fields $h_i \in [h_0 - \epsilon, h_0 + \epsilon]$. We will further restrict ourselves to $h_0 = 1.25$ for specificity—$h_0 = 1.25, J = 0.95$ gives good chaotic level statistics for small systems in the Hermitian limit. (The Hermitian model has been used as a "generic" chaotic model, see e.g. [50].) Eq. (7) has a special line at $\gamma = 1$, along which σ_i^x and σ_i^y form the raising operator σ_i^+. Consequently, H is an upper triangular matrix and its eigenvalues are precisely its diagonal entries. Since these diagonal entries are real (up to the offset), this solvable line must lie in the mixed phase, consistent with our numerics and mean-field theory.

The phase diagram of the clean model ($\epsilon = 0$) is plotted in Fig. 1. The extent of the mixed phase is non-monotonic, with purification happening soonest when $J \approx h_0/2$. This matches the mean-field prediction: at $J = h_0/2$, the applied longitudinal field exactly cancels the self-generated mean field at the transition. Past a critical decay rate, the pure phase arises from a sequence of exceptional points that appear in increasingly close proximity to each other with increasing system size [39].

In the mixed phase, $\Pi(t)$ stabilizes to some finite long-time value [Fig. 2(a)], with oscillations whose period and amplitude grow as one approaches the transition; in the

pure phase $\Pi(t)$ quickly approaches unity. Moreover, the bipartite entanglement of an initially pure state grows to an apparent volume law in the mixed phase [Fig. 2(b)]—though its growth is very slow near the transition [39]—but in the pure phase it seems to saturate at an area law. To access the long-time limit, we must proceed differently in the two phases. In the mixed phase, following Eq. (3), one can construct a time-averaged density matrix $\rho_{\rm ss}$ starting from the identity. $\rho_{\rm s.s.}$ has volume law Rényi entropies throughout the mixed phase, with coefficients that decrease as the transition is approached [Fig. 2(c)]. The spectrum of $\rho_{\rm ss}$ has a power-law tail [39], which explains the very different volume-law coefficients of S_∞ and S_1. In the pure phase, any initial state gets projected onto the longest-lived eigenvector; for $\gamma = 1.1$ the entanglement entropy of this extremal state (which a generic initial state approaches) is clearly area-law [Fig. 2(d)].

We now turn to the properties of the eigenvalues and eigenstates of the Hamiltonian (7), which (distinctively) the present setup gives us access to. The eigenvalue statistics are illustrated in Fig. 2(e). We characterize these via the level-statistics ratio $r \equiv \min(|\lambda_i - \lambda_{i-1}|, |\lambda_{i+1} - \lambda_i|)/\max(|\lambda_i - \lambda_{i-1}|, |\lambda_{i+1} - \lambda_i|)$ [51]. (We add weak quenched randomness to the longitudinal field, with a bandwidth $\epsilon = 0.05 \ll h_0$, to break any residual spatial conservation laws; the exact value of ϵ does not affect our results.) In the mixed phase, all eigenvalues have the same imaginary part so eigenvalue differences are purely real. For a chaotic real Hamiltonian, $\langle r \rangle \approx 0.53$ while for a localized or integrable Hamiltonian, $\langle r \rangle \approx 0.39$ (Poisson level statistics). We find that even for moderately large γ, r is close to its value in the Hermitian limit. Nearer to the transition, however, level repulsion gets weaker, and the level spacing ratio dips toward the Poisson value. This dip does not appear to be a finite-size effect: the histogram of r appears well converged with respect to system size. At $\gamma = 1$, the eigenvalues are just the diagonal entries of the Hamiltonian, and their level spacing is manifestly Poisson.

Finally, we turn to the eigenstates. For small γ, these are qualitatively similar to those in the Hermitian limit: almost all eigenstates in the middle of the spectrum are highly entangled, whereas those near the spectral edge have low entanglement. Eigenstates at similar energies have similar entanglement properties, as dictated by the eigenstate thermalization hypothesis. As γ increases, however, nearby eigenstates begin to have large variations in their entanglement [Fig. 2(f)], signaling the breakdown of eigenstate thermalization. Nevertheless, the average half-cut eigenstate entanglement continues to scale as a volume law in this regime. A generic initial pure state, after dephasing, becomes a random-phase superposition of these eigenstates, and correspondingly also exhibits volume-law entanglement.

As already noted, a crucial feature of eigenvectors in the non-Hermitian case is that they are not mutually orthogonal. Although any state can be expressed as a superposition of eigenvectors, a generic random-phase superposition of these can be efficiently approximated by a vector in a much lower-dimensional space. Thus the matrix P transforming the computational basis into the eigenbasis can be well approximated by a lower-rank matrix P'. We estimate the needed rank of P' in terms of the participation ratio of the list of singular values of P, which scales as $2^{-\alpha(\gamma)L}$ where $\alpha \equiv (\log_2 P')/L$ decreases from unity in the Hermitian limit to approximately 0.64 at the transition. Notably, some distance away from the transition, α is very close to the entropy density s_1 of the time-averaged density matrix [Fig. 2(c)].

Discussion.—The central result of this work is that an entanglement transition can occur, with no spatial or temporal randomness, via the breaking of PT symmetry in an interacting many-body system under continuous measurement. This PT-symmetry breaking seems different from that in random circuits—e.g., it happens even for a two-level system—but the phase structure of the problems is qualitatively similar. In both cases, there is a phase in which an initially mixed density matrix stays mixed—but with reduced entropy—and an initial product state acquires volume law entanglement, and a phase where an initially mixed state purifies and a product state only develops area-law entanglement. While (to our knowledge) the model (7) and its transition have not been discussed, other many-body exceptional points exist [44–46], and it would be interesting to study them from the entanglement perspective developed here.

The flow of quantum information under non-Hermitian time evolution is an interesting question to explore. The coefficients of the initial state in the eigenbasis become very large to capture the behavior along the dimensions approximately "missing" from the eigenbasis. Under time evolution, this initial state dephases and is rotated into the (lower-dimensional) space that is efficiently spanned by the eigenvectors. However, the information carried by the late-time state is determined by its large coefficients along the "missing" dimensions. The implications of this dynamics for encoding and retrieving quantum information remain to be understood. It would be interesting, e.g., to adapt the theory of entanglement domain walls [16, 18, 24, 52, 53] to non-Hermitian quantum mechanics: because our system lacks quenched randomness, we expect these domain walls to have qualitatively different properties than in random circuits with measurements, so the subleading correction to volume law entanglement in the mixed phase should differ.

This work marks an initial foray into studying entanglement in post-selected, non-Hermitian quantum mechanics, which, as we have shown, is rich enough to capture entanglement transitions that are distinct from both the many-body localization transition in unitary dynamics and the measurement transition in random unitary-projective dynamics. We have not addressed

whether there are practical protocols to realize these effects in near-term devices. The probability of the no-measurement evolution occurring in a system of size L for a time t scales exponentially with Lt, so achieving the long-time limit for a large system is inaccessible. However, locally detectable *crossovers* associated with this transition should occur on finite timescales [54]. Viewed from the angle of quantum complexity theory, post-selected quantum mechanics is known to encompass a much broader complexity class than conventional quantum mechanics [55]. As a result, there may be fundamental information-theoretic barriers to universal realizations of non-Hermitian quantum mechanics. Whether these arguments prohibit efficient simulations of specific models, such as the ones studied in this paper, remains an outstanding question.

Note added.—While this work was being completed, Ref. [35] was posted. Both works discuss non-Hermitian phase transitions but otherwise the models and results do not overlap.

We thank Chris Hooley, David Huse, Vedika Khemani, and Vadim Oganesyan for helpful discussions and collaborations on related topics. M.J.G also thanks Yidan Wang and Alexey Gorshkov for helpful discussions. We thank Emily Townsend for helpful comments on the manuscript. This work was supported by the National Science Foundation under NSF Grant No. DMR-1653271.

[1] H.-P. Breuer, F. Petruccione, *et al.*, *The theory of open quantum systems* (Oxford University Press on Demand, 2002).
[2] G. Schaller, *Open quantum systems far from equilibrium*, Vol. 881 (Springer, 2014).
[3] I. Rotter and J. Bird, Reports on Progress in Physics **78**, 114001 (2015).
[4] S. Diehl, A. Micheli, A. Kantian, B. Kraus, H. P. Büchler, and P. Zoller, Nat. Phys. **4**, 878 (2008).
[5] J. Dalibard, Y. Castin, and K. Mølmer, Physical review letters **68**, 580 (1992).
[6] V. Gorini, A. Kossakowski, and E. C. G. Sudarshan, J. Math. Phys. **17**, 821 (1976).
[7] G. Lindblad, Commun. Math. Phys. **48**, 119 (1976).
[8] Y. Li, X. Chen, and M. P. A. Fisher, Phys. Rev. B **98**, 205136 (2018).
[9] B. Skinner, J. Ruhman, and A. Nahum, Phys. Rev. X **9**, 031009 (2019).
[10] A. Chan, R. M. Nandkishore, M. Pretko, and G. Smith, Phys. Rev. B **99**, 224307 (2019).
[11] Y. Li, X. Chen, and M. P. A. Fisher, Phys. Rev. B **100**, 134306 (2019).
[12] M. J. Gullans and D. A. Huse, arXiv e-prints , arXiv:1905.05195 (2019), arXiv:1905.05195 [quant-ph].
[13] M. J. Gullans and D. A. Huse, Phys. Rev. Lett. **125**, 070606 (2020).
[14] R. Fan, S. Vijay, A. Vishwanath, and Y.-Z. You, arXiv e-prints , arXiv:2002.12385 (2020), arXiv:2002.12385 [cond-mat.stat-mech].
[15] S. Choi, Y. Bao, X.-L. Qi, and E. Altman, arXiv e-prints , arXiv:1903.05124 (2019), arXiv:1903.05124 [quant-ph].
[16] C.-M. Jian, Y.-Z. You, R. Vasseur, and A. W. W. Ludwig, arXiv e-prints , arXiv:1908.08051 (2019), arXiv:1908.08051 [cond-mat.stat-mech].
[17] X. Cao, A. Tilloy, and A. D. Luca, SciPost Phys. **7**, 24 (2019).
[18] Y. Bao, S. Choi, and E. Altman, Phys. Rev. B **101**, 104301 (2020).
[19] A. Nahum and B. Skinner, arXiv e-prints , arXiv:1911.11169 (2019), arXiv:1911.11169 [cond-mat.stat-mech].
[20] A. Zabalo, M. J. Gullans, J. H. Wilson, S. Gopalakrishnan, D. A. Huse, and J. H. Pixley, Phys. Rev. B **101**, 060301 (2020).
[21] Q. Tang and W. Zhu, Phys. Rev. Research **2**, 013022 (2020).
[22] J. Lopez-Piqueres, B. Ware, and R. Vasseur, arXiv e-prints , arXiv:2003.01138 (2020), arXiv:2003.01138 [cond-mat.stat-mech].
[23] Y. Li, X. Chen, A. W. W. Ludwig, and M. P. A. Fisher, arXiv e-prints , arXiv:2003.12721 (2020), arXiv:2003.12721 [quant-ph].
[24] Y. Li and M. P. A. Fisher, arXiv e-prints , arXiv:2007.03822 (2020), arXiv:2007.03822 [quant-ph].
[25] A. Lavasani, Y. Alavirad, and M. Barkeshli, arXiv e-prints , arXiv:2004.07243 (2020), arXiv:2004.07243 [quant-ph].
[26] S. Sang and T. H. Hsieh, arXiv e-prints , arXiv:2004.09509 (2020), arXiv:2004.09509 [cond-mat.stat-mech].
[27] O. Alberton, M. Buchhold, and S. Diehl, arXiv e-prints , arXiv:2005.09722 (2020), arXiv:2005.09722 [cond-mat.stat-mech].
[28] M. Ippoliti, M. J. Gullans, S. Gopalakrishnan, D. A. Huse, and V. Khemani, arXiv preprint arXiv:2004.09560 (2020).
[29] M. Ippoliti and V. Khemani, arXiv preprint arXiv:2010.15840 (2020).
[30] L. Fidkowski, J. Haah, and M. B. Hastings, arXiv preprint arXiv:2008.10611 (2020).
[31] A. Nahum, S. Roy, B. Skinner, and J. Ruhman, arXiv preprint arXiv:2009.11311 (2020).
[32] J. Iaconis, A. Lucas, and X. Chen, arXiv preprint arXiv:2010.02196 (2020).
[33] T. E. Lee and C.-K. Chan, Phys. Rev. X **4**, 041001 (2014).
[34] J. P. Garrahan and I. Lesanovsky, Phys. Rev. Lett. **104**, 160601 (2010).
[35] A. Biella and M. Schiró, arXiv preprint arXiv:2011.11620 (2020).
[36] A. Polkovnikov, K. Sengupta, A. Silva, and M. Vengalattore, Rev. Mod. Phys. **83**, 863 (2011).
[37] R. Nandkishore and D. A. Huse, Annual Review of Condensed Matter Physics **6**, 15 (2015), https://doi.org/10.1146/annurev-conmatphys-031214-014726.
[38] A. Chan, A. De Luca, and J. T. Chalker, Phys. Rev. X **8**, 041019 (2018).
[39] See online supplemental material.
[40] C. M. Bender and S. Boettcher, Physical Review Letters **80**, 5243 (1998).
[41] N. Moiseyev, *Non-Hermitian quantum mechanics* (Cam-

bridge University Press, 2011).
[42] Y. Takasu, T. Yagami, Y. Ashida, R. Hamazaki, Y. Kuno, and Y. Takahashi, arXiv preprint arXiv:2004.05734 (2020).
[43] Y. Ashida, Z. Gong, and M. Ueda, arXiv preprint arXiv:2006.01837 (2020).
[44] Y. Ashida, S. Furukawa, and M. Ueda, Nature communications **8**, 1 (2017).
[45] Y. Ashida, K. Saito, and M. Ueda, Physical review letters **121**, 170402 (2018).
[46] R. Hanai and P. B. Littlewood, Physical Review Research **2**, 033018 (2020).
[47] D. Roscher, S. Diehl, and M. Buchhold, Phys. Rev. A **98**, 062117 (2018).
[48] J. Huber, P. Kirton, and P. Rabl, Phys. Rev. A **102**, 012219 (2020).
[49] J. Huber, P. Kirton, S. Rotter, and P. Rabl, SciPost Physics **9**, 052 (2020).
[50] H. Kim and D. A. Huse, Physical review letters **111**, 127205 (2013).
[51] V. Oganesyan and D. A. Huse, Phys. Rev. B **75**, 155111 (2007).
[52] C. Jonay, D. A. Huse, and A. Nahum, arXiv e-prints , arXiv:1803.00089 (2018), arXiv:1803.00089 [cond-mat.stat-mech].
[53] T. Zhou and A. Nahum, Phys. Rev. X **10**, 031066 (2020).
[54] J. M. Hickey, E. Levi, and J. P. Garrahan, Phys. Rev. B **90**, 094301 (2014).
[55] S. A. Aaronson, Proc. R. Soc. A **461**, 3473 (2005).